

⁵Leung, Y.T., "An Accurate Method of Dynamic Condensation in Structural Analysis," *International Journal of Numerical Methods in Engineering*, Vol. 12, 1978, pp. 1705-1715.

⁶Paz, M., "Dynamic Condensation," *AIAA Journal*, Vol. 22, May 1984, pp. 724-727.

Strength Prediction of a Mechanically Fastened Joint in Laminated Composites

Charles E.S. Ueng* and Kai-da Zhang†
Georgia Institute of Technology, Atlanta, Georgia

Introduction

RECENTLY, advanced composites have been widely used in many aerospace structures. Just as in any structure made of conventional materials, a load must be transmitted from one member to another through an efficiently and effectively designed joint. This is particularly important for composite structures because any weight saving through the use of modern composites can be easily eroded by improper or overdesigned joints. Mechanically fastened joints can provide certain advantages, such as ease of inspection, no need for special surface treatment, and tolerance to the effects of environmental loading. The authors^{1,2} have recently obtained compact analytical solutions, including the frictional effect, for the stresses around a pin-loaded hole by stress functions of complex variables. The results indicate that, in general, the normal stress does not follow a cosinusoidal distribution for orthotropic material and the presence of friction may cause a significant effect to the stress distribution. In this Note, those solutions^{1,2} are used for computing the stresses along a characteristic curve^{3,4} and then the Yamada-Sun⁵ criterion is applied to evaluate the ultimate load and the failure mode. The results are compared with the available experimental data.⁶⁻⁸

The advantages of this approach are: 1) the effect of the friction on the strength prediction is included; 2) the strength evaluation of a mechanical joint involving an arbitrarily orthotropic composite material can be carried out without complicated computation as long as the basic material properties are given; and 3) the method is easily adaptable for the case where the direction of the pin load does not coincide with the direction of one of the material principal axes.²

Analysis

The following assumptions are made for deriving a simple and reasonable prediction of the failure pin load: 1) only two-dimensional stress analysis is considered and the effect of delamination is ignored; 2) the laminate is bonded perfectly; 3) distribution of the pin load along the plate thickness is uniform; and 4) a final failure occurs when a combination of stresses in any lamina of this laminate reaches the critical value. The Yamada-Sun criterion is used to predict the ultimate strength, that is,

$$(\sigma_{xi}/X)^2 + (\tau_i/S_c)^2 = \ell^2 \begin{cases} \ell^2 < 1, \text{ no failure} \\ \ell^2 \geq 1, \text{ failure} \end{cases} \quad (1)$$

Received Sept. 7, 1984; revision received March 4, 1985. Copyright © American Institute of Aeronautics and Astronautics, Inc., 1985. All rights reserved.

*Professor, Engineering Science and Mechanics.

†Instructor, Northwestern Polytechnical University, Xian, Shaanxi, China.

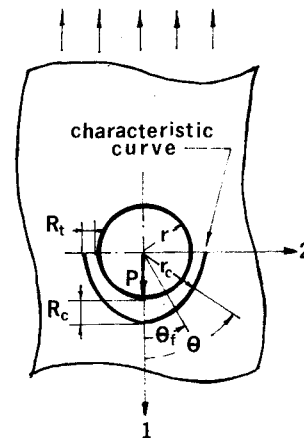


Fig. 1 A sketch of the characteristic curve ($D=2r$).

where σ_{xi} and τ_i are the normal stress along the direction of fiber and the shear stress in the i^{th} lamina, respectively, X the ply longitudinal strength, and S_c the ply shear strength measured from a symmetric cross-ply laminate. It is noted that σ_{xi} and τ_i are the stresses at points located on a characteristic curve whose equation is represented by

$$r_c = r + R_t + (R_c - R_t)\cos\theta, \quad -\pi/2 \leq \theta \leq \pi/2 \quad (2)$$

as shown in Fig. 1, where r is the radius of the loaded hole and R_t and R_c the characteristic lengths determined from experimental results. They depend only on the material itself.

For the strength prediction, we adopt the following approach in which the stress values around a loaded hole are multiplied by the ratio r/r_c in order to obtain the stresses around the characteristic curve. The reason is that the characteristic curve is located nearby the hole and the elasticity effect of this small region between the hole edge and the characteristic curve can therefore be ignored. In doing so, the tedious computational work can be avoided. Based upon this approximation, the stresses around the characteristic curve can be simply presented as

$$\sigma_{rc} = \sigma_r r / r_c, \quad \sigma_{\theta c} = \sigma_{\theta} r / r_c, \quad \tau_{r\theta c} = \tau_{r\theta} r / r_c \quad (3)$$

where σ_r , σ_{θ} , and $\tau_{r\theta}$ are the normal stresses and shear stress around the pin-loaded hole, respectively. The detailed computational procedure and equations are available in Ref. 9.

Comparison with Experimental Results

The following constants adopted from Refs. 3, 4, and 10 are used in the evaluation of the failure load: $R_c = 2.032$ mm (0.08 in.), $R_t = 0.457$ mm (0.018 in.); friction coefficient $f = 0.2$, and $S_c = 2.5S$ where S represents the lamina shear strength obtained by testing single plies. The predicted failure mode is determined as suggested by Chang et al.³ as follows:

$-15 < \theta_f < 15$ deg, bearing failure mode

$30 < \theta_f < 60$ deg, shearout failure mode

$75 < \theta_f < 90$ deg, tension failure mode

where θ_f is the angle for a point where the combined stress reaches the critical value. Tables 1-3 list the experimental and analytical results for the failure loads or stresses of two kinds of laminates made of the same fiber but with different matrix materials. (Note: All of the tests quoted in Tables 1-3 were made at room temperature and under static load up to failure.)

For considering the effect caused by friction, the ultimate bearing strengths for some laminates are calculated under dif-

ferent coefficients of friction. The results are presented in Fig. 2. The ultimate strengths of laminates containing two different stacking sequences with different percentages of proportion are also calculated. For all cases, the friction coefficient is taken as 0.2. Such results are shown in Figs. 3 and 4. The dotted curves included in Figs. 3 and 4 are taken from Ref. 11.

Discussion of Results

The values of R_c and R_t as given in Ref. 4 were adopted for the purpose of estimating the failure loads for all three kinds of laminates considered. This is based upon the fact that all of them are made of the same type of fiber, but different matrix materials. Their orthotropic parameter ratios such as k and n do not differ very much.⁹ From the comparison of the results, the error runs 1-30% for most cases. It should be pointed out, however, that such a wide deviation in the strength prediction is not infrequent in the literature.

An interesting outcome of the analytical solution obtained here is that the presence of friction can increase the failure load in certain cases. It is perhaps the friction force that changes the failure mode for certain laminates. For example, the inclusion of friction will reduce the maximum value of σ_r , which is to the benefit of the bearing strength; and if the residual shear strength of the laminates is high enough, a change of the failure mode will increase the ultimate failure load. But for any further increase of the friction force, it will reduce the failure load. For different laminates, the effect of friction is also different.

Collings¹¹ observed that, in certain cases, a different percentage of orientations could increase the bearing strength.

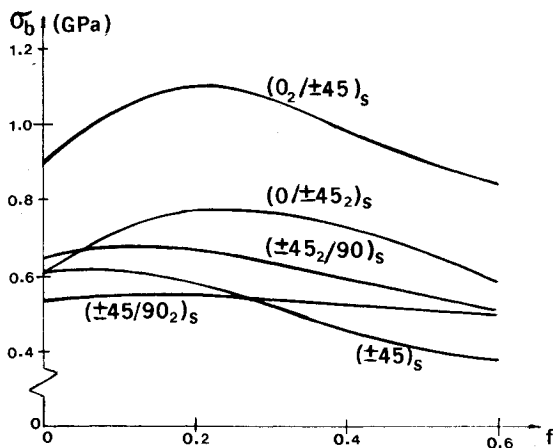


Fig. 2 Effect of friction to the bearing strength (T300/5208).

There is a similar trend shown in our results, although the degree of increase differs somewhat (Figs. 3 and 4). Since the analytical stress results used in this Note are derived from an infinite plate case, it should be expected that the analytical prediction is more satisfactory for failure modes such as bearing or shearout than the net tension mode and for the case where the ratios W/D and e/D are large enough.

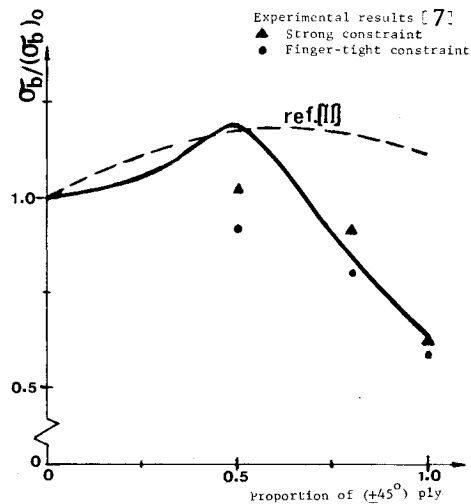


Fig. 3 Bearing strength of $(0^\circ/\pm 45^\circ)$ laminates.

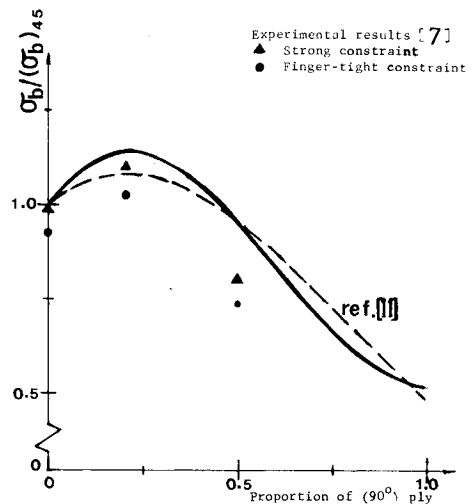


Fig. 4 Bearing strength of $(90^\circ/\pm 45^\circ)$ laminates.

Table 1 Comparison of experimental and analytical results for T300/SP 286⁶ ($f=0.2$, hole diameter = 0.476 cm)

| No. | Laminates ^a | | | | Analytical | | | Experimental | | |
|-----|-------------------------|-------|-------|------------------|---------------------|-----------------------------------|---------------------------|---------------------|--------------|-----------------------|
| | Stacking sequence | W/D | e/D | Ultimate load, N | Initial failure ply | Failure position θ_f , deg | Failure mode ^b | Av. failure load, N | Failure mode | Error, ^c % |
| 1 | $(0/\pm 45/90)_s$ | 5.34 | 2.98 | 4150 | 0 | 20 | B/SO | 4982 | NT | 17 |
| 2 | $(0/\pm 45/90)_s$ | 8.02 | 4.01 | 4150 | 0 | 20 | B/SO | 5137 | B | 19 |
| 3 | $(0/\pm 45/90)_s$ | 8.02 | 2.98 | 4150 | 0 | 20 | B/SO | 4804 | B/SO | 14 |
| 4 | $(0/\pm 45/90)_s$ | 8.02 | 2.04 | 4150 | 0 | 20 | B/SO | 4226 | SO | 2 |
| 5 | $(0/\pm 45/90)_s$ | 5.34 | 2.04 | 8693 | 0 | 20 | B/SO | 8562 | NT/SO | -1.5 |
| 6 | $(0\pm 45/90/\pm 45)_s$ | 5.34 | 2.98 | 5507 | 0 | 20 | B/SO | 7517 | NT | 26.7 |
| 7 | $(0_2/\pm 45/90)_s$ | 5.34 | 2.98 | 4705 | 45 | 60 | SO | 6094 | SO | 23 |
| 8 | $(\pm 45)_{2s}$ | 5.34 | 2.98 | 2423 | 45 | 30 | SO | 3914 | NT | 38 |
| 9 | $(0/90)_{2s}$ | 5.34 | 2.98 | 2934 | 0 | 50 | SO | 3002 | SO | 2 |
| 10 | $(0_2/\pm 45)_{2s}$ | 5.34 | 2.98 | 4731 | 45 | 60 | SO | 4363 | B/SO | -8.4 |

^a W = width of the specimen, e = distance from the center of the hole to the end of the specimen, $D = 2r$ = diameter of the hole. ^b Failure mode: NT = net tension failure, SO = shearout failure, B = bearing failure. ^c Error = $(N_{exp} - N_{anal.}) \times 100 / N_{exp}$.

Table 2 Comparison of experimental and analytical results for T300/5208⁷ ($f=0.2$, hole diameter = 0.635 cm, $W/D=4$, $e/D=3$)

| No. | Laminates | Analytical | | | | Experimental I ^a | | | Experimental II | | |
|-----|-------------------------------------------|------------------|---------------------|------------------------------------|--------------|-----------------------------|--------------|----------|---------------------|--------------|----------|
| | | Ultimate load, N | Initial failure ply | Failure position, θ_f , deg | Failure mode | Av. failure load, N | Failure mode | Error, % | Av. failure load, N | Failure mode | Error, % |
| 1 | (± 45) _s | 12290 | -45 | 40 | SO | 11410 | NT | -7.7 | 12180 | NT | -1.0 |
| 2 | (0/ ± 45) _s | 14080 | 0 | 30 | SO | 13370 | NT | -5.3 | 15440 | NT | 8.0 |
| 3 | (0 ₂ / ± 45) _s | 23340 | 45 | 50 | SO | 17940 | B | -30.1 | 19980 | 45°(NT) | -16.8 |
| 4 | ($\pm 45_2/90$) _s | 12030 | 45 | 30 | SO | 10600 | NT | -13.5 | 11480 | NT | -4.8 |
| 5 | ($\pm 45/90_2$) _s | 11720 | 45 | 30 | SO | 9123 | Nt | -28.5 | 9961 | NT | -17.7 |

^aFor experimental results I, constraint torque of bolt = 0.56 N.m (5 lb.in.); for II, torque = 8.4 N.m (75 lb.in.).

Table 3 Comparison of experimental and analytical results for T300/5208⁸ ($f=0.2$, hole diameter = 0.3175 cm, $W/D=8$, $e/D=6.5$)

| No. | Laminates | Analytical | | | | Experimental ^{8 a} | | Experimental ⁷ | |
|-----|---------------------------------------------|-------------|---------------------|------------------------------------|--------------|-----------------------------|----------|---------------------------|-------------|
| | | Stress, MPa | Initial failure ply | Failure position, θ_f , deg | Failure mode | Stress, MPa | Error, % | Stress, MPa | Error, % |
| 1 | (0 ₂ / ± 45) _{2s} | 1096 | 45 | 50 | SO | 586.7 | -86.8 | 842.6/938.4 ^a | -30.1/-16.8 |
| 2 | (90 ₂ / ± 45) _{2s} | 554.2 | 45 | 30 | SO | 515.7 | -7.5 | 431.4/471.1 | -28.5/-17.7 |
| 3 | (0/90/ ± 45) _{2s} | 876.5 | 0 | 20 | B/SO | 619.7 | -41.4 | | |

^aSee the footnote of Table 2 for the two different cases.

Experimental data obtained by Collings¹¹ and Wilkins⁷ indicated that the failure load of a bolted joint with strong lateral constraint is 10-20% higher than the finger-tight case. A strong lateral constraint tends to limit the delamination possibility of a laminate, which is physically equivalent to the assumption that no consideration is given for delamination. This is confirmed by an overall small error percentage given under II and I in Table 2.

In a realistic structure, the direction of pin load may not coincide with one of the principal directions of a laminate. This can be handled without any difficulty by employing the results recently obtained by the authors² in connection with the same method adopted in this Note. In addition, considerations such as environmental effects and nonlinear and/or inelastic behavior would have to be included in the practical strength prediction of a bolted joint. The procedure and the results presented here can potentially reduce the number of tests that otherwise would be needed for the strength prediction of a mechanically fastened joint in laminated composites.

References

- ¹Zhang, K.D. and Ueng, C.E.S., "Stresses Around a Pin-loaded Hole in Orthotropic Plates," *Journal of Composite Materials*, Vol. 18, 1984, pp. 432-446.
- ²Zhang, K.D. and Ueng, C.E.S., "Stresses Around a Pin-loaded Hole in Orthotropic Plates with Arbitrary Loading Direction," *International Journal of Composite Structures*, Vol. 3, 1985, pp. 119-143.
- ³Chang, F.K., Scott, R.A., and Springer, G.S., "Strength of Mechanically Fastened Composite Joints," *Journal of Composite Materials*, Vol. 16, 1982, pp. 470-494.
- ⁴Chang, F.K., Scott, R.A., and Springer, G.S., "Strength of Bolted Joints in Laminated Composites," AFWAL-TR-844029, March 1984.
- ⁵Yamada, S.E. and Sun, C.T., "Analysis of Laminate Strength and Its Distribution," *Journal of Composite Materials*, Vol. 12, 1978, pp. 275-284.
- ⁶Agarwal, B.L., "Static Strength Prediction of Bolted Joints in Composite Material," *AIAA Journal*, Vol. 18, 1980, pp. 1371-1375.
- ⁷Wilkins, D.J., "Environmental Sensitivity Tests of Graphite-Epoxy Bolt Bearing Properties," *Composite Materials: Testing and Design*, ASTM STP 617, 1977, pp. 497-513.
- ⁸Kim, R.Y. and Whitney, J.M., "Effect of Temperature and Moisture on Pin Bearing Strength of Composite Laminates," *Journal of Composite Materials*, Vol. 10, 1976, pp. 149-155.

⁹Ueng, C.E.S. and Zhang, K.D., "Strength Prediction of a Mechanically Fastened Joint in Laminated Composites," AIAA Paper 85-0823, April 1985.

¹⁰Hyer, M.W. and Klang, E.C., "Stresses Around Holes in Pin-loaded Orthotropic Plates," *Proceedings of 25th AIAA/ASME/ASCE/AHS Structures, Structural Dynamics & Materials Conference*, AIAA, NY, May 1984, pp. 232-242.

¹¹Collings, T.A., "On the Bearing Strength of CFRP Laminates," *Composites*, Vol. 13, 1982, pp. 241-252.

Dynamic Response of Orthotropic, Homogeneous, and Laminated Cylindrical Shells

A. Bhimaraddi*

University of Melbourne, Victoria, Australia

Introduction

RECENT developments in the analysis of plates and shells laminated of fiber-reinforced materials indicate that thickness has more pronounced effects on the behavior of composite laminated shells than on isotropic laminated shells. Also, due to low transverse shear moduli relative to in-plane Young's moduli, transverse shear deformation effects are even more pronounced in composite laminates. Reliable prediction of the response characteristics of high modulus composites therefore requires the use of shear deformation theories.

Several theories to analyze laminated shells have been put forward in which the effects of transverse shear deformation are taken into account. The first formulation of such a theory for orthotropic laminated cylindrical shells appears to be due to Dong and Tso.² Similar works on laminated shells can be found in Refs. 3-5. An exposition of various shell theories is

Received June 10, 1983; revision received Nov. 27, 1984. Copyright © by A. Bhimaraddi. Published by the American Institute of Aeronautics and Astronautics with permission.

*Department of Civil Engineering.